DIELECTRIC AND OPTICAL PROPERTIES
OF TIN- DOPED BARIUM TETRA TITANATE CERAMICS

ASAD ALI[1] *, SARIR UDDIN [2], ABID ZAMAN[1], ABID AHMAD[1], MUHAMMAD KAMRAN[3], ZAFAR IQBAL[1]
[1]Department of Physics, Riphah International University, Islamabad 44000, Pakistan
[2]Department of Physics, Government Degree College Hayatabad, Peshawar 25000 Pakistan
[3]Department of Electronics, University of Peshawar 25000, Pakistan

Solid solution of Tin- doped barium tetra titanate $Ba(Ti_{1-x}Sn_x)_4O_9$ (with x = 0.0, 0.5) composition prepared through mixed oxide conventional method and calcined at 1100˚C for 3 h with heating/cooling rate 5˚C/min. The structural, optical and microwave dielectric properties were studied by X-ray diffraction, Scanning electron microscopy, Fourier transform infra-red, photoluminescence spectroscopy and vector network analyzer respectively. An intense and broad band spectrum was observed at around the red color emission region. Optimum dielectric properties i.e. high dielectric constant (ϵ_r = 57.3) and low dielectric loss (0.00013) have been observed.

Keywords: Mixed oxide route, Optical properties, Dielectric properties

1. Introduction

Barium titanate ceramics, like barium tetra titanate ($BaTi_4O_9$) material, have wide applications in microwave (mw) telecommunication technologies e.g. global positioning system (GPS), satellite broadcasting, cellular phones and air traffic control system [1]. The main objective of recent research in this field is to design new ceramics material or to modify the mw dielectric properties i.e. high dielectric constant (ϵ_r), near to zero temperature coefficients of resonant frequency (τ_f) and low dielectric loss (tanδ) of already known ceramic materials. Masse et al reported low dielectric loss barium tetra titanate (BT4) dielectric resonator (DR) for the first time at early 1970's [2]. BT4 play a vital rule in the breakthrough in the mw-wireless communication or dielectric ceramics technology. BT4 samples had been fabricated through conventional mixed oxide route using horizontal milling of the mixtures of reactants $BaCO_3$ and TiO_2 for 24 h [3, 4]. Cernea et al obtained BT4 samples from wet chemical method and recorded dielectric constant (37), dielectric loss (0.0017) and temperature coefficient of resonant frequency (11ppm/°C [5]. The structural, optical and mw dielectric properties of BT4 samples with several different additives have also been investigated in the microwave region [6-9]. Many studies have been carried out on the substitution in the B site. Some of them have reported on the influence of the substitution of Sn^{4+} ions for Ti^{4+} ions [10-12]. Veenhuis et al reported that BT4 based samples showed favorable applications in the field of electronic or optical storage devices, advance laser technologies etc. [13].

The main objective of this work is to synthesize and characterize low loss dielectrics with improved dielectric and optical properties through studying the effects of substituting Sn^{4+} for Ti^{4+} in $Ba(Ti_{1-x}Sn_x)_4O_9$ (with x = 0.0, 0.5) composition.

2. Experimental procedures

The solid solution of barium tetra titanate $Ba(Ti_{1-x}Sn_x)_4O_9$ (with x = 0.0, 0.5) composition was obtained by conventional mixed oxides route. The starting raw materials were analytical grade high-purity (99.9%) oxide powders, $BaCO_3$ (Merck, Germany), TiO_2 (Aldrich Chemical Company, Inc., U.S.A) and SnO_2 (Strem, Chemicals, U.S.A). Stoichiometric amounts of the oxides were weighed according to composition and ball-mixed for 24 h in distilled water (wetting media). The mixture was dried in an oven at 90 °C for 24 h in air and the dried mixture was calcined in high purity alumina crucible at 1100 °C for 3 h in air at 5 °C/min heating/cooling rate in conventional furnace to yield $[Ba(Ti_{1-x}Sn_x)_4O_9]$ (with x = 0, 0.5) powders. The calcined mixtures were grinded manually with a mortal and pistol for 12 h to avoid agglomeration. The fine powders were pressed into pellets of 10 mm in diameter and 5 mm thick under a pressure of 7 ton/in² using a manual pellet press (CARVER, USA). The pellets samples were sintered at temperatures of 1320 °C for 2 h in air with 5 °C/min heating/cooling rate. The crystalline phases of the calcined ceramics samples were identified by using X-rays diffractometer (XRD) (JDX-3532, JEOL, Japan) with Cu Kα (λ = 0.15406 nm) radiation operated at 40 mA and 40 kV in a wide range of Braggs angles 2θ (10° < 2θ < 90°) at scanning rate of 2°/min. The experimental densities of the samples were calculated using Electronic Densimeter (MD-3005). The morphological studies of the sintered sample were carried out using scanning electron microscopy (SEM, JEOL 7600F)

---

* Autor corespondent/*Corresponding author*,
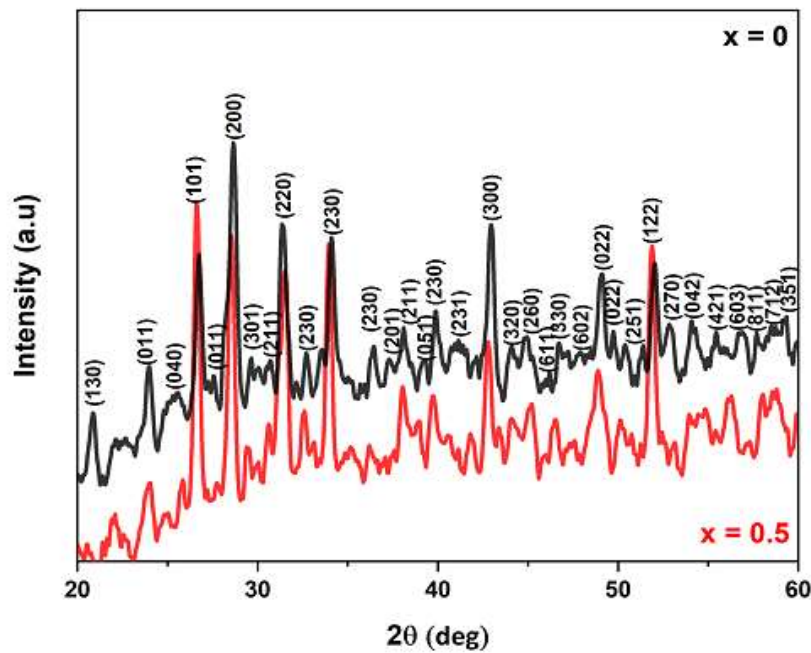E-mail: kasadiiui@gmail.com

Fig 1 - XRD patterns of Ba(Ti$_{1-x}$Sn$_x$)$_4$O$_9$ (with x = 0.0, 0.5) calcined at 1100 °C for 3 h.

Table 1

Crystallite size of each plane for BT4 sample.

Planes	Brags angle (2θ) (degree)	Brags angle (θ) (degree)	FWHM (β) (radian)	Crystallite size (D) (nm)
(130)	20.85	10.42	0.0071	19.88
(011)	23.91	11.95	0.0068	20.84
(200)	28.54	14.27	0.0065	21.71
(220)	31.41	15.70	0.0096	15.0
(230)	33.96	16.98	0.0057	25.43
(300)	42.80	21.4	0.005	29.74
(122)	51.80	25.9	0.011	14.03

operated at 15 kV. The Fourier transformation infrared spectroscopy (FTIR) absorption spectrum was recorded on a Perkin-Elmer GX FTIR system was used to obtain 10 cm^{-1} resolution spectrum in the range 400 to 4000 cm^{-1} region. The photo-luminescence spectroscopy (PL) spectrum was recorded on a Jobin Yvon-Horiba Triax 190 spectrometer with 0.30 nm resolution spectrum. The dielectric properties of sintered ceramic samples were measured by using vector network analyzer (ZVB20, Rohde & Schwarz, Germany).

3 Results and discussions
3.1 Structural analysis

Figure 1 shows the XRD patterns of the Sn-doped barium tetra titanate (BaTi$_4$O$_9$) calcine at 1100 °C for 3hrs in air and undoped barium tetra titanate. The XRD patterns show that they are all single phase orthorhombic structures (which can be indexed as BaTi$_4$O$_9$) and matched with JCPDS card # 34-70, with space group Amm2 [14]. These results demonstrated that with the replacement of Ti^{4+} by Sn^{4+}, Ba(Ti$_{1-x}$Sn$_x$)$_4$O$_9$ (with x = 0.0, 0.5)

composition would form a solid solution. It has also been observed that the positions of the diffraction peaks of the ceramics shift slightly to lower angle with increasing Sn^{4+} content in the range of 2θ from 42 to 50°. This is attributed to the larger ionic radius of Sn^{4+} (0.069nm) as compared having that of Ti^{4+} (0.060 nm) with results in a slight enlargement of crystal cell volumes and hence a shift of diffraction peaks towards lower angles. The crystallite size of each major peak can be calculated by using the Debye Scherer's formula [15] and observed approximately 21.0 nm average crystallite size as shown in Table 1.

$$D = \frac{0.9\lambda}{\beta Cos\theta} \qquad \text{Eq. (1)}$$

Where 'D' is the crystallite size, 'λ' is the wavelength of Cu Kα radiation, 'θ' is the brags angle and 'β' is the full-width at half-maximum (FWHM). The average crystallite size of BT4 sample was reported to be 15.0 nm [16].

The change in orthorhombic to tetragonal structure was observed at composition x = 0.5 as shown in Table 2.

Table 2

Physical properties of Ba(Ti$_{1-x}$Sn$_x$)$_4$O$_9$ (with x = 0.0, 0.5) ceramics

Sample	structure	ϵ_r	(ρ_{th}), (gm/cm^3)	(ρ_{ex}), (gm/cm^3)	(ρ_{re}), (%)	Porosity (%)
BaTi$_4$O$_9$	Orthorhombic	24.28	4.41	4.21	95.6	4.53
Ba(Ti$_{0.5}$Sn$_{0.5}$)$_4$O$_9$	Tetragonal	57.3	5.73	5.61	97.9	2.1

ρ_{th} = theoretical density, ρ_{ex} = experimental density, ρ_{re} = relative density ϵ_r = dielectric constant.
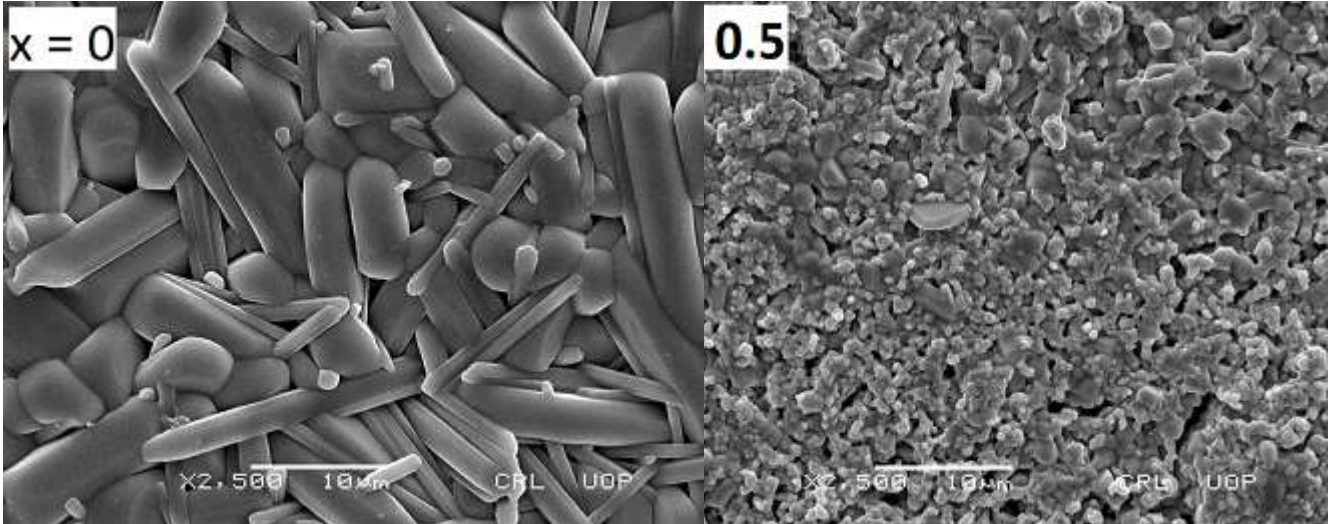

Fig 2 - SEM Micrograph for x = 0 and x = 0.5 in the system of Ba(Ti$_{1-x}$Sn$_x$)$_4$O$_9$ sintered ceramic at 1320 °C for 2 h.

3.2 Microstructure analysis

The secondary electron images (SEIs) with different resolutions, from thermally etched and gold-coated Ba(Ti$_{1-x}$Sn$_x$)$_4$O$_9$ (with x = 0.0, 0.5) ceramic samples sintered at 1320 °C for 2 hrs is shown in Fig 2. Both the samples are dense and have varying microstructural features with the presence of cavities. The presence of cavities in the SEM images shows that the pellets have a certain amount of porosity. The grain boundaries and grain size can be seen very clearly in a non-agglomerated region and the grain size reduces with increasing Sn^{4+} content. Porosity can be decreased by increasing the relative density of the sample [17]. We have calculated the porosity of the samples using equation (2) and observed small value of porosity at x = 0.5 Sn^{4+} content as shown in Table 2.

$$\text{Porosity} = \left(\frac{\rho_{th} - \rho_{ex}}{\rho_{th}}\right) \times 100\% \qquad \text{Eq. (2)}$$

Densification further induced by Sn^{4+} content (x = 0.5) which tends to reduce the grain growth [18]. This increase in density is also evident in SEM microstructures images and decreasing of porosity was shown in Table 2.

3.3 Optical properties

Figure 3 shows the FTIR pattern of fabricated compound Ba(Ti$_{1-x}$Sn$_x$)$_4$O$_9$ (with x = 0.0, 0.5) ceramic material. A strong absorption peak appears near 466, 1437 and 2926 cm^{-1}. According to the previous research about the titanates [19], these peaks characterize the vibration of Ti-O
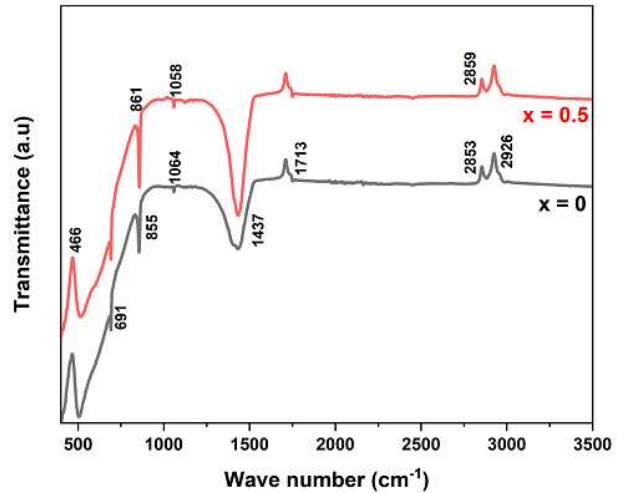

Fig 3 - FTIR spectra of Ba(Ti$_{1-x}$Sn$_x$)$_4$O$_9$ (with x = 0.0, 0.5) calcined ceramic at 1100 °C for 3 h

octahedron. The wavenumber of absorption peak of pure BaT$_4$O$_9$ is 855 and 2853 cm^{-1}. It can be changed by tin (Sn) additives to 861 and 2859cm^{-1} respectively. Dazhi Sun et al [20] reported that only one O-vacancy can be produced by replacing Ba^{2+} and three O-vacancies are produced by replacing Ti^{4+} by means of respective additives. In this way Ti-O octahedrons are damaged or distorted easily. Several vibrations modes were observed in the FTIR spectrum. Therefore, the comparative study of the FTIR spectra further supports the improvement of redispersibility of the polycrystalline barium tetra titanate dielectric material.

Photoluminescence (PL) spectra of $Ba(Ti_{1-x}Sn_x)_4O_9$ (with x = 0, 0.5) calcined ceramic at 1100 °C for 3 h excited with 488 nm laser beam source at room temperature shown in Figure 4. PL spectra of sample material have defected related deep level emission in the visible region of the optical spectrum. The emission in the visible region is recognized to the recombination of holes and electron in the state of delocalization. This state of delocalization is due to the intrinsic structural defect related to Ti^{4+} microcrystal symmetric in the micro phase of $BaTi_4O_9$. The PL emission spectra of the sample is recorded red color (604.6 nm) with excitation energy (2.05 eV) at x = 0 content and (605.8 nm) with excitation energy (2.04 eV) at x = 0.5 content respectively. This red color represented the electronic transition generated by different degrees of structural order-disorder in sample [21]. PL is a typical multiphoton process that is an emission occurred in optical energy gape by many vibrational states within it. This can be confirmed that PL is directly associated with the existing localized state within the band gape which affected the structural order-disorder directly.
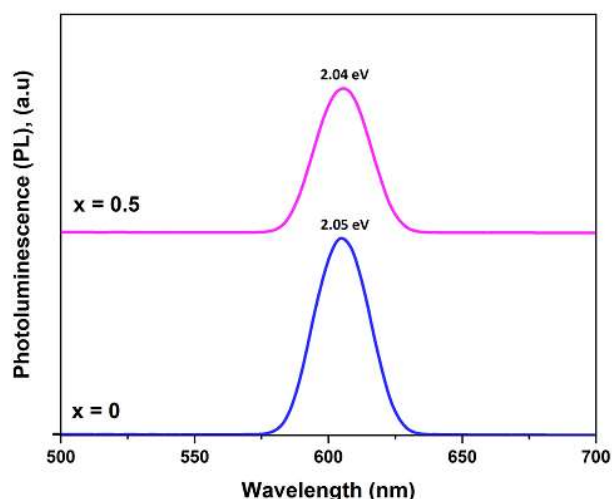

Fig 4 - PL spectra of $Ba(Ti_{1-x}Sn_x)_4O_9$ (with x = 0.0, 0.5) calcined ceramic at 1100 °C for 3 h

Therefore, the structural order increases with increasing the band gape energy [22]. It has been observed that a broad emission band is located at ~604.6 nm and has excitation energy (~2.05 eV) smaller than the band gap energy of highly ordered barium tetra titanate located at ~558 nm (~2.23 eV) which is due to the oxygen vacancy [23]. In this PL characteristic oxygen vacancy act is a red color emitted source.

3.4 Microwave dielectric properties
The dielectric constant (ϵ_r) and dielectric loss (tan δ) in the frequency range of 100MHz–800MHz of $Ba(Ti_{1-x}Sn_x)_4O_9$ (with x = 0.0, 0.5) sintered ceramic at room temperature is shown in Figures 5. It can be seen that the value of dielectric constant at x = 0.5 content which is higher than

that of x = 0 content. The relative permittivity of both samples is almost remaining constant with increasing frequency. The increase in the relative permittivity due to Sn doping may be as the result of decreasing the grain size and increasing the densification of the sample. Dielectric loss of the sample increases exponentially with increasing frequency. In the region of lower frequency, a decrease in the value of dielectric loss was observed which is due to the dominance of space charge polarization and orientational charge polarization of the sample [24]. We have observed optimum dielectric properties at x = 0.5 content.
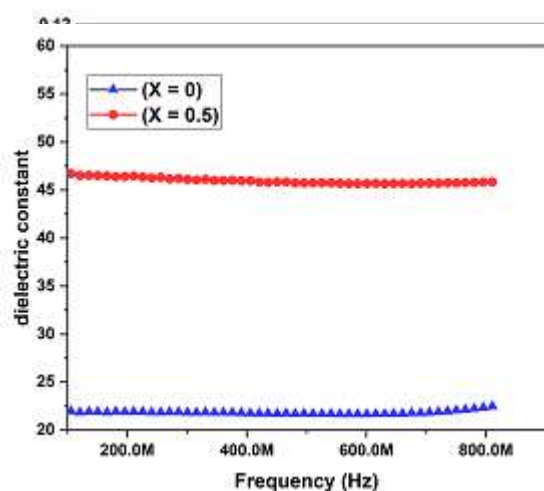

Fig 5 - Variation of dielectric loss and dielectric constant vs. frequencies of $Ba(Ti_{1-x}Sn_x)_4O_9$ (with x = 0.0, 0.5) sintered ceramic at 1320 °C for 2 h.

4. Conclusion

Lead free solid solution of $Ba(Ti_{1-x}Sn_x)_4O_9$, (with x = 0.0, 0.5) were fabricated through conventional mixed oxide route and their microwave dielectric properties were developed. The conclusions were followed as
1. Well polycrystalline $BaTi_4O_9$ ceramics could be prepared by the mixed oxide route and average crystallite size of 21 nm was observed from XRD peaks.
2. The XRD pattern revealed that the sample has orthorhombic structure at x = 0 and Tetragonal structure at x = 0.5 composition.
3. Sintered ceramics achieved a 97.7% theoretical density at x = 0.5 and well grain growth.
4. The dielectric properties of sintered ceramics samples showed high dielectric constant (ϵ_r = 57.3) and low dielectric loss (tanδ = 0.00013).

REFERENCES

[1] M. T. Sebastian, in *Dielectric materials for wireless communication*, Elsevier B.V, Great Britain: 1st edition, (2008).

[2] D. J. Masse, R. A. Pucel, D. W. Readey, E. A. Maguire and C. P. Hartwig. *Proceedings of the IEEE*. 1971, 59 (11), 1628-1629.

[3] S. G. Mhaisalkar, W. E. Lee and D. W. Readey. *J. Am. Ceram. Soc.* 1989, 72 (11), 2154–2158.

[4] S. G. Mhaisalkar, D. W. Readey and S. A. Akbar. *J. Am. Ceram. Soc.* 1991, 74 (8), 1894–1898.

[5] M. Cernea, E. Chirtop, D. Neacsu et al. *Journal of the American Ceramic Society*. 2002, 85 (2), 499–503.

[6] S. G. Mhaisalkar, D. W. Readey, S. A. Akbar et al. *J. Solid State Chem.* 1991, 95 (2), 275-284.

[7] S. Nishigaki, S. Yano , H. Kato et al. *J. Am. Ceram. Soc.* 1988, 71 (1), C-11-C17.

[8] V. Ern and R. E. Newnham. *J. Am. Ceram. Soc.* 1961, 44 (4), 199-205.

[9] S. G. Mhasalkar, W. E. Lee and D. W. Readey. *J. Am. Ceram. Soc.* 1989, 72 (1), 2154-2160.

[10] V. Mueller, H. Beige, and H. P. Abicht, *Appl. Phys. Lett.* 2004, 84, 1341

[11] S.G. Lu, Z.K. Xu, and H. Chen, *Appl. Phys. Lett.* 2004, 85, 5319

[12] V.V. Shvartsman, W. Kleemann, J. Dec, Z.K. Xu, and S.G. Lu, *J. Appl. Phys*. 2006, 99, 124111

[13] H. Veenhuis et al. *J. Appl. Phys.* 2002, 70 (6), 797-801.

[14] Y. B. Chen and S. S. Liu. *Journal of Materials Science: Materials in Electronics*. 2019, 30, 5567–5572

[15] A. L. Patterson. *Phys. Rev.* 1939, 56, 978-986.

[16] J. Tao *et al. Mater. Res. Bull.* 2008, 43, 639-645.

[17] S. Mahajan et al. *J. Bull. Mater. Sci.* 2011, 34 (7), 1483–1489.

[18] T. A. Naboulsia, M. Boulos, C. Tenailleau, P. Dufour, M. Zakhour, G. F. Sophie. *Journal of Ceramic Processing Research*. 2016, 17(8), 870-875

[19] C. H. Perry and B. N. Khanna, *Phys. Rev.* 1957, 105, A408

[20] D. Sun et al. J. *Ferroelectrics*. 2007, 355:145–148,

[21] V. M. Longo, L. S. Cavalcante, A. T. Figueiredo et al. *Appl. Phys. Lett.*, 2007, 90, 906-911.

[22] E. R. Leite, E. C. Paris, F. M. Pontes et al. *J. Mat. Sci.* 2003, 38, 1175-1183.

[23] M.E. Marssi, F. L. Marrec, I. A. Lukyanchuk et al. *J. Appl. Phys.* 2003, 94, 3307-3316.

[24] S. Gattu, K. S. Dasari, V. R. Kocharlakota. *World Journal of Condensed Matter Physics*. 2015, 5, 346-352.

****